Polymer Chemistry

Accepted Manuscript

This is an *Accepted Manuscript*, which has been through the Royal Society of Chemistry peer review process and has been accepted for publication.

Accepted Manuscripts are published online shortly after acceptance, before technical editing, formatting and proof reading. Using this free service, authors can make their results available to the community, in citable form, before we publish the edited article. We will replace this *Accepted Manuscript* with the edited and formatted *Advance Article* as soon as it is available.

You can find more information about *Accepted Manuscripts* in the Information for Authors.

Please note that technical editing may introduce minor changes to the text and/or graphics, which may alter content. The journal's standard Terms & Conditions and the Ethical guidelines still apply. In no event shall the Royal Society of Chemistry be held responsible for any errors or omissions in this *Accepted Manuscript* or any consequences arising from the use of any information it contains.

ROYAL SOCIETY OF CHEMISTRY

www.rsc.org/polymers

Journal Name

ARTICLE

Interpenetrating Poly(urethane-urea)-Polydimethylsiloxane Networks Designed as Active Elements in Electromechanical Transducers

Received 00th January 20xx,
Accepted 00th January 20xx

DOI: 10.1039/x0xx00000x

www.rsc.org/

C. Tugui, [a] S. Vlad, [a] M. Iacob, [a] C.D. Varganici[a], L. Pricop and M. Cazacu[a]

A poly(urethane-urea-siloxane), was prepared in a two-steps procedure consisting in the synthesis of bis-isocyanate prepolymer on the basis of 4,4'-diphenylmethane diisocyanate, a polyether glycol and dimethylol propionic acid, and its extending by reacting with 1,3-bis(3-aminopropyl)tetramethyldisiloxane. The resulted polymer was used in different percentages to prepare three series of interpenetrating networks (IPNs) with polydimethylsiloxane-α,ω-diols with molecular masses, Mn, of 70000, 230000 and 370000 g·mol^{-1}. A polydimethylsiloxane–polyethyleneoxide graft copolymer, was added as compatibilizing agent. The IPN precursors were mixed in solution and processed as films. During solvent evaporation, the chemical crosslinking of the polydimethylsiloxane-α,ω-diols occurs with tetraethylorthosilicate in presence of dibutyltin dilaurate, while in the case of poly(urethane-urea-siloxane) only physical crosslinking by hydrogen bonds is expected to occur. The morphology of the resulted networks was examined by scanning electron microscopy and differential scanning calorimetry and dynamic mechanical analysis. The mechanical and dielectric characteristics (dielectric permittivity, loss, strength) of the aged films were studied. Their responsiveness to an external stimulus in form of increasing electric field was assessed by electromechanical measurements and expressed as lateral strain. The results were critically analyzed in relation to each other as in correlation with their composition and compared with those obtained for three usual dielectric elastomers commercially available.

Introduction

Dielectric elastomers, soft materials, are a subgroup of electroactive polymers, generally used in electromechanical transducers due to their capabilities to respond to electrical stimuli.[1,2] When a potential difference is applied across the electrodes, the induced charge causes an electrostatic attraction between these. The resulting compressive force, or Maxwell stress, leads to a reduction in film thickness, which in turn results in an expansion in the plane of the film.[1] Given their valuable properties, this class of materials has enabled the development of new and interesting applications such as power generators,[3,4] energy harvesting,[5] sensors,[6] artificial muscles,[7] etc. After a large number of elastomers were screened for such applications, only three classes of materials were identified as the most promising: silicones, polyurethanes and acrylics.[8-13] However, none of them meets all performance criteria (low Young modulus, low plastic deformation, high elongation at break, high breakdown strength, high dielectric permittivity and low fabrication cost) for such applications. The commercially available 3M VHB acrylic elastomer (VHB4910 and VHB4905) appears to be most promising in terms of actuation strain performance, with strains in excess of 380 % reported for highly prestrained films. The theoretical estimated energy density of this elastomer is very high, 3.4 J·cm^{-3}, while the coupling coefficient as well as efficiency can reach 90 %.[14,15] However, these show high viscoelastic losses. Polyurethanes have high dielectric permittivity which is based on the polar nature of the polyurethane fragments (roughly 7, compared to 3 for silicones[16]) allowing them to be actuated at lower electric fields but cannot develop large strains.[14] However, the high polarity of polyurethanes can lead to a slightly increased sensitivity towards humidity; low concentration of chemical cross-links in the thermoplastic polyurethane (TPU), as well as in the acrylate, result in a high level of creep or permanent deformation of these materials under actuation strain.[16] Thus, although polyurethanes were initial considered promising, the interest for them lowered after obtaining significant improvements in the actuation properties of prestrained silicone and acrylic films, the main research being now focused mainly on polyurethane-based composites.[14,17] For a commercial silicone (Nusil CF19-2186) it was found the highest energy density and strain among the elastomer tested.[18] Silicone elastomers are capable of strain over 100 % when prestrained although they are under the acrylic advantage in this regard, but have viscoelastic losses lower than acrylics. In addition, they have better coupling efficiency, low creep and can operate in a wide temperature range without significantly alter their characteristics. These made the most far developed actuators to be on the basis of silicones.[18] But silicones have relative low dielectric constant thus requiring large electric fields to be actuated.[19] Therefore, new formulations of commercially available elastomers

"Petru Poni" Institute of Macromolecular Chemistry, Iasi, 700487, Romania.
E-mail: mcazacu@icmpp.ro.
† Footnotes relating to the title and/or authors should appear here.
Electronic Supplementary Information (ESI) available: [details of any supplementary information available should be included here]. See DOI: 10.1039/x0xx00000x

that to combine in a single material their performance and to limit their shortcomings are being developed continuously.[14]

Analysing the above, in this paper we considered polyurethanes and silicones from the perspective of designing a new material suitable for electromechanical applications. Polyurethanes are generally synthesized by polyaddition reaction of isocyanates with alcohols. The building blocks of polyurethane may be separated into the hard segments, such as the urethane group, and soft ones mainly based on polyether polyol (C2–C4) or polyester (aliphatic or aromatic).[20] These fragments can have significantly different dipole moments. Thus, the huge versatility of their chemistry, which, at least in theory, allows almost unlimited combinations to create the polymers with desired properties, make the polyurethanes a very suitable candidate for dielectric elastomers (DE) development from this point of view.[16] The introduction of the dimethylsiloxane segments within polyurethane backbone could reduce intermolecular connection, increase the chain flexibility and reduce the glass transition and also improve the compatibility with nonpolar components such as silicones. Only a few examples in which the soft segment is siloxane one are reported.[21]

In this paper we prepared an original polyurethane containing tetramethyldisiloxane moieties but also carboxyl groups in structure. This was used as a component to prepare interpenetrated bi-networks with polydimethylsiloxane-α,ω-diols with various molecular masses. Networks interpenetration is a promising technique of preparing materials with broad glass transition temperature (Tg) ranges[16] and offers the possibility of effectively producing advanced multi-component polymeric systems with new properties profiles. The mutual entangling forces the compatibilization of the two networks leading to a dual-phase continuous microstructure in systems with synergistic effects. While polydimethylsiloxane chains were crosslinked, the polyurethane networks self-stabilized by hydrogen bonds between their own polar groups. Thus prepared networks, after aging, were structurally characterized and investigated from point of view of the thermal and moisture behaviour. The mechanical and dielectric characteristics and electromechanical actuation were evaluated. The results were compared with those measured in the same conditions for three commercially available dielectric elastomers: silicone (Sylgard 186), acrylic (VHB 3M 4910) and a natural rubber. Besides expected improving of certain features, interpenetration of the silicone with polyurethane networks creates prerequisites for getting a material with reduced costs given that polyurethanes are cheaper than silicones.

Experimental section

Materials

The following materials were used for polyurethane preparation: a polyether glycol Terathane®, (PTMEG, average molecular weight 2000 g·mol^{-1}) offered for free by Invista BV Netherland while dimethylol propionic acid (DMPA), 4,4'-diphenylmethane diisocyanate (MDI), dimethylformamide (DMF) and dibutyltin dilaurate (DBTL) were purchased from Sigma-Aldrich; 1,3-bis(3-aminopropyl)tetramethyldisiloxane, BATD, and tetraethylorthosilicate (TEOS) were purchased from Alfa Aesar GmbH & Co KG, Germany. PTMEG was checked for moisture and, if was necessary, it was lowered at 0.3 %. Rests of chemicals were used as received without further purifications. The polydimethylsiloxane–polyethyleneoxide graft copolymer, PDMS-g-PEO, was prepared by hydrosilylation reactions of the α-allyl,ω-acetate-polyethyleneoxide (molecular weight around 2000 g·mol^{-1}) with polysiloxane copolymer containing around 10 mol% Si-H groups, according to reference.[22] The composition of graft copolymer, as determined on the basis of ^{1}H NMR spectroscopy: 18 mol % methyl(ethylene oxide)siloxane units and 82 mol % dimethylsiloxane units. The molecular mass, Mn, as determined by gel permeation chromatography (GPC) by elution with DMF, was 11000 g·mol^{-1} (I=1.1). Surface tension in 1.0% aqueous solution – 37.3 mN·mm^{-1}. Polydimethylsiloxane-α,ω-diols (PDMS) with molecular masses of 230000 and 370000 g· mol^{-1} were prepared by cationic ring-opening polymerization of octamethylcyclotetrasiloxane catalysed by sulphuric acid according to procedures described in reference.[23] The PDMS of molecular mass of 70000 g·mol^{-1} was prepared by bulk cationic ring-opening polymerization in the presence of cation exchanger Purolite CT-175.[23]

Sylgard® 186 silicone from Dow Corning, VHB 4910 from 3M and the natural rubber sample were used as films.

Measurements

FTIR was used to examine changes in the molecular structures of the samples after mixing. The spectra were measured on a Bruker Vertex 70 FT-IR instrument, equipped with a Golden Gate single reflection ATR accessory, spectrum range 600-4000 cm^{-1}, at ambient temperature. ^{1}H NMR spectra were recorded on a Bruker Advance III 400 MHz spectrometer, using DMSO as solvent.

The morphology of the films was studied by scanning electron microscope (ESEM) type Quanta 200 operating at 20kV with secondary and backscattering electrons in low vacuum mode.

Differential scanning calorimeter (DSC) 200 F3 Maia (Netzsch, Germany) was used for thermal behaviour measurements. About 10 mg of sample was heated in pressed and punched aluminum crucibles at a heating rate of 10 °C·min^{-1}. A flow rate of 100 mL·min^{-1} of nitrogen was used as inert atmosphere.

Dynamic mechanical analysis (DMA) was performed on a PerkinElmer instrument in tension mode. The test specimens were 14 mm long, 8.5 mm wide and 0.24 mm thick. The samples were scanned with a heating rate of 2 °C·min^{-1} between -150 °C and -25 °C in a single frequency (1Hz), under nitrogen atmosphere.

Water vapors sorption capacity of the film samples was measured by using the fully automated gravimetric analyser IGAsorp supplied by Hiden Analytical, Warrington (UK). An ultrasensitive microbalance measuring the weight change as the humidity is modified in the sample chamber at a constant regulated temperature. The measurement system is controlled by a IGASORP Windows™ based software package.

Stress–strain measurements were performed on dumbbell-shaped cut from thin films on a TIRA test 2161 apparatus, Maschinenbau GmbH Ravenstein, Germany. Measurements were run at an extension rate of 50 mm·min^{-1}, at room temperature. All

samples were measured three times and the averages were obtained.

Novocontrol setup (Broadband dielectric spectrometer Concept 40, GmbH Germany), integrating an ALPHA frequency response analyser and a Quatro temperature control system, with working frequency range 10^0-10^6 Hz, at room temperature was used for the determination of the dielectric behaviour.

The breakdown voltage measurements were carried out on a home-built setup.[19] The experiments were performed by applying a ramp signal of 500 V·s^{-1} from a Trek 20/20C-HS power generator on the IPN sample, which has been placed between two unequal electrodes: a planar ground electrode having 150 mm in diameter and a high voltage electrode having a 5 mm diameter and a spherical surface. The electrical voltage applied on the IPN membranes was measured by using a HV probe connected to a digital oscilloscope.

Actuation measurements were performed on circular membranes fixed between two circular frames. Circular electrodes of 10 mm in diameter based on carbon grease were applied on both sides of the film and a Trek 20/20C-HS amplifier was used as power supply. An AFG 3000 wave generator was used to generate a symmetric rectangular signal. In order to perform the actuation measurements, the voltage was raised from 0 to the required actuation voltage in about 10 ns and maintained for 2.5 s. The actuation strain was determined optically, by measuring the extension of the electrode via a digital camera, using a software program to determine the electrode diameter.[24]

Procedure

Preparation of poly(urethane-urea-siloxane), PUUS

Firstly, 0.01 mol of PTMEG and 0.01 mol of DMPA were dehydrated under vacuum (1-2 mmHg), at 80 °C for 2 h and stirred (120 rpm). Then, under normal conditions of pressure, 30 mL DMF was added as a solvent. After complete dissolution, 0.03 mol MDI and 2-3 drops DBTL as catalyst were added. The mixture was stirred at 80 °C for 2 h, when a homogenous prepolymer was obtained. When viscosity increases, was added a new quantity of DMF (up to 40 mL), under same conditions. In the next step, the prepolymer was extended. For this, the reaction medium was cooled at 0 °C, and then 80 mL of BATD solution in DMF was slowly added in about 1 h. Then, the stirring was continued for 1 h with progressive temperature up to 80 °C, until the polymer solution becomes clear.

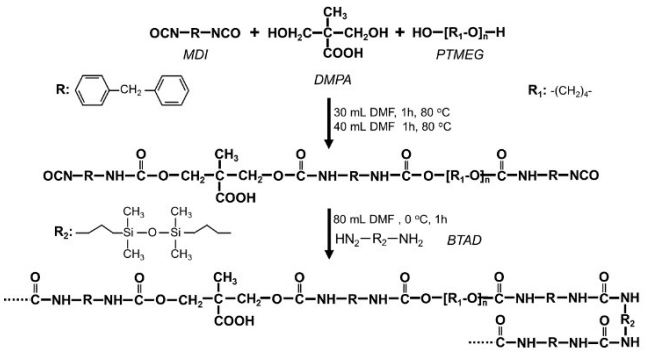

Scheme 1. The synthetic route to poly(urethane-urea-siloxane) having carboxyl groups pending on the main chain.

Afterwards, the siloxane-containing poly(ether-urethane-urea) with carboxyl groups in the main chain was precipitated in hot distilled water (45-50 °C) and then allowed to cool. The polymer was washed for few times with distilled water to remove the solvent, and then dried under vacuum for several days. The molar ratio of reactants (MDI: PTMEG: DMPA: BATD) was of 3: 1: 1: 1. Scheme 1 presents the synthesis pathway to poly(urethane-urea siloxane), PUUS, with carboxyl groups on main chain.

IR (KBr): 3295w (NH stretching vibration), 2942m (aliphatic C-H antisymmetric stretch), 2858m (aliphatic C-H symmetric stretch), 1731m (urethane –C=O vibration), 1661m (urea –C=O vibration), 1596m (aromatic ν(C=C)), 1536m (NH in plane bending), 1410w, 1369w and 1309w (CH_2 and CH_3 bending vibrations), 1224m (ν(C-N) and δ(NH) (amide III) of aliphatic –R-NH-COO-), 1105s (-C-O-C- stretching vibration), 1063s (Si-O-Si asymmetric stretch), 817m (Si-CH_3 rocking mode), 755w (Si-CH_2- rocking mode).[25-27]

^{1}H NMR (400 MHz, DMSO-d6, δ, ppm): 9.56 (COOH), 8.34 (N-H), 7.09-7.38 (-C_6H_4-), 3.77 (-C_6H_4-*CH_2*-C_6H_4-), 3.38 (-O-CH_2), 3.06 (-*CH_2*-CH_2-CH_2-Si-) 1.49 (CH_2, CH_2), 1.22 (-CH_2-*CH_2*-CH_2-Si-), 0.48 (-CH_2-CH_2-*CH_2*-Si-), 0.07 ($(CH_3)_2$Si-O-).[26]

Preparation of poly(urethane-urea-siloxane)-polydimethylsiloxane interpenetrated networks, PUUS-PDMS IPNs

The PUUS obtained as above was mixed with each of the three PDMSs in amounts as showed in Table 1. For these, the two precursors, PDMS and PUUS were separated solved in THF and DMF, respectively and stirred for 48 h at room temperature and then were mixed together for another 8 h. Then 0.2 ml as a solution 10 wt% PDMS-g-PEO in THF was added and the mixture was stirred again for one hour. In the end, 0.14 mL TEOS and two drops DBTL were added and the mixture was vigorously stirred for 15 min, after which was degassed by ultrasonication for five minutes and poured as film on a Teflon substrate and left to cure at room temperature for 48 h. For each molecular mass of silicones, a reference sample consisting in pure PDMS crosslinked with TEOS and 1 wt% PDMS-g-PEO in presence of DBTL was prepared. A film only on the basis of physically crosslinked PUUS was also cast. All films were aged for one month in laboratory environmental conditions before to be analysed.

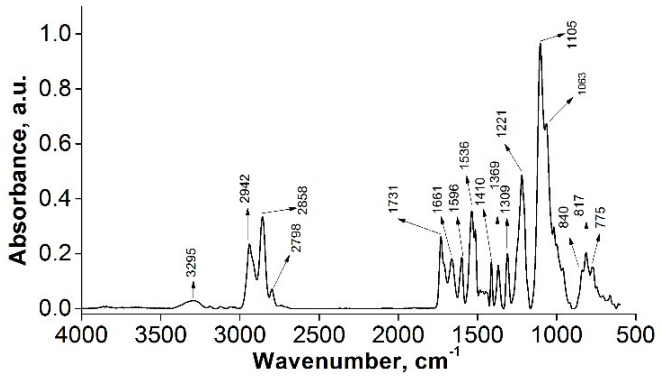

Figure 1. FTIR spectrum of poly(urethane-urea-siloxane), PUUS.

Table 1. Amounts of precursors used for the synthesis of IPNs (0.20 ml PDMS-g-PEO, 10 wt% solution in THF, 0.14 mL TEOS, two drops DBTL).

Sample	Polymeric precursors for IPNs X, PDMS, Mn=70000 g·mol^{-1} [g]	Y, PDMS, Mn=230000 g·mol^{-1} [g]	Z, PDMS, Mn=370000 g·mol^{-1} [g]	PU, 10% sol in DMF [mL]
PUUS	0	0	0	20
X-0%	2	0	0	0
X-5%	2	0	0	1
X-10%	2	0	0	2
X-20%	2	0	0	4
Y-0%	0	2	0	0
Y-5%	0	2	0	1
Y-10%	0	2	0	2
Y-20%	0	2	0	4
Z-0%	0	0	2	0
Z-5%	0	0	2	1
Z-10%	0	0	2	2
Z-20%	0	0	2	4

Results and discussions

First, a poly(urethane-urea-siloxane), PUUS, was prepared in a two-step procedure consisting in the synthesis of bis-isocyanate prepolymer on the basis of 4,4'-diphenylmethane diisocyanate (MDI), a polyether glycol (PTMEG) and dimethylol propionic acid (DMPA), and its extending by reacting with 1,3-bis(3-aminopropyl)tetramethyldisiloxane (BATD) in molar ratio of 3:1:1:1. (Scheme 1). Both polycondensation steps occurred in solution in DMF. The polymer separated by precipitation, repeated washing with water and drying, was characterized by spectral (FTIR and ^{1}H NMR) methods.

The absence of the band at about 2230 cm^{-1} in FTIR spectrum of PUUS suggests complete consumption of the isocyanate, NCO, groups. Their reaction with hydroxyl leads to the formation of urethane linkage, while the reaction with amine group results in urea bond. The presence of these bonds in the formed structure is well emphasized by FTIR spectrum (Figure 1) where the specific absorption bands at 1661 cm^{-1} (NH-CO-NH), 3295 cm^{-1} (NH) and 1731 cm^{-1} (urea and urethane C=O), are present. The Si-O-Si bond presence in structure is proved by the band at 1063 cm^{-1}.[25-27]

In ^{1}H NMR spectrum (Figure S1) are present the peaks characteristic for all types of protons, according to the proposed structure.[26]

Thus obtained PUUS was interpenetrated with three polydimethylsiloxane-α,ω-diols with different molecular masses, Mn: 70000, 230000, 370000 g·mol^{-1}. Three weight percentages (5, 10, 20 wt%) of polyurethane as solution in DMF were added to the silicone solution in THF. An in house-prepared silicone surfactant PDMS-g-PEO based on the short chain silicone modified with α-allyl,ω-acetate-polyethyleneoxide was added each time in the same small amount (0.2 mL as a solution 10 % in THF) to contribute, besides the amphiphile, mixed nature of polyurethane, to good compatibility between the two networks, PUUS and PDMS. TEOS and DBTL were used as crosslinker and catalyst, respectively. Reference samples based on crosslinked PDMS only containing surfactant and also physical crosslinked simple PUUS were prepared and used as references to evaluate the changes in the properties occurring in IPNs.

All mixtures were processed as films, cured and aged at room temperature in laboratory environmental conditions. During curing, the crosslinking of the PDMS occurs by condensation of the Si-OH end groups with TEOS catalysed by DBTL, while the polyurethane networks stabilizes by formation of the physical intermolecular bonds (hydrogen bonds presumed to be, in principal) both between polyurethane chains or these and PEO segments of surfactant (Scheme 2).

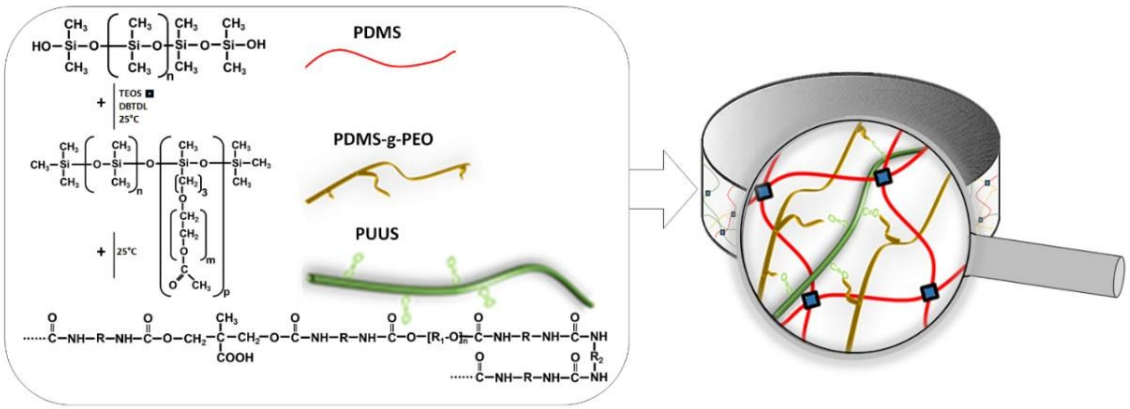

Scheme 2. Graphical representation of the IPNs formation.

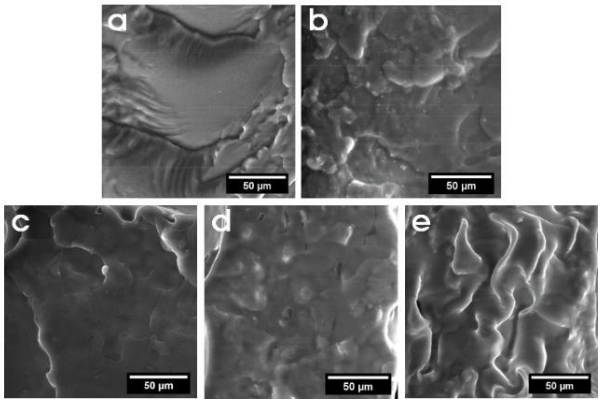

Figure 2. SEM images of: a - PUUS; b - Y-0%; c - Y-5%; d - Y-10%; e - Y-20%.

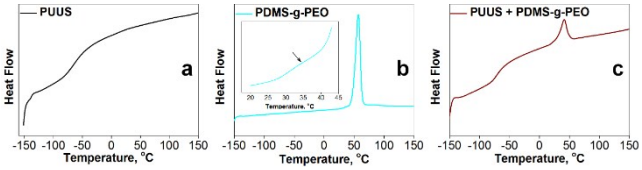

Figure 3. DSC curves of: a - pure PUUS; b - PDMS-g-PEO; c - PUUS/ PDMS-g-PEO system.

Morphology of films

The morphology of the obtained IPN films was studied by scanning electron microscopy (SEM) in cryo-fractured section. While the simple PUUS show a monophasic morphology (Figure 2a), in the case of the sample Y-0% based on PDMS with addition of PDMS-g-PEO, spherical aggregates are visible that are assigned to the surfactant (Figure 2b). A structuration is also visible in the case of the IPN films in all cases (Figure 2c,d,e) with larger domains when compared with pure crosslinked PDMS. This mainly consists in spherical domains of micrometre order. A porosity of the films created by the late solvent/by-products evaporation was observed on SEM images taken on surface (Figure S2).

Thermal behaviour

DSC is a versatile analytical tool, offering crucial insights regarding solid state interactions, with emphasis on phase separation phenomena, usually confirmed by microscopy studies. During the obtaining of semi– or interpenetrating polymer networks there occurs a synergism effect of the individual comprising components properties by a forced phase compatibilization. This leads to reciprocal compensation of properties between system components.[28] In general, complete phase compatibilization of polymers is reached when the system exhibits a single glass transition temperature (Tg) domain.[19] The structure of PUUS having many polar groups along the chain permits physical crosslinking in higher degree as compared with long polydimethylsiloxane chains, chemically crosslinked through ends only. This makes the PUUS's Tg peak being too flat to be easily seen observed in DSC. Thus, a Tg domain centered at –65 °C with a very low heat flow value of

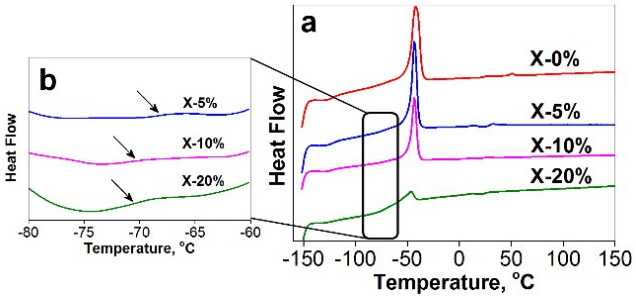

Figure 4. DSC curves of: a - series **X** networks; b - corresponding Tg domains zoom.

0.112 mW·mg^{-1} (Figure 3a, Figure S6, Table 2) was identified for individual polyurethane (PUUS). The more solid, rigid and brittle textured PDMS-g-PEO structure presented a significantly weak Tg value at 35 °C and an intense melting profile at 57 °C with an enthalpy (ΔH) value of 110.4 J·g^{-1} (Figure 3b, Table 2). Because the PEO content in PDMS-g-PEO is majority, their transitions determine the pattern of DSC curve, those for siloxane segment being difficult to identify. Series X shows a first Tg value raging between –119 and –121 °C, correspond to PDMS (Figure 4, Table 2).[10] A second Tg but weaker (Figure 4b) ranging between –68 and –71 °C was evidenced through DSC by zoom scans, in the case of IPNs and attributed to PUUS component. Series Y and Z manifested similar behaviour (Table 2, Figures S3 and S4). Measurements by DMA revealed about the same values for Tg as those found by DSC, illustrative curves being showed in Figure S5. The presence of two Tg domains suggests phase separation phenomenon occurrence.[10] However, the extremely weak Tg value of PUUS and the absence of PDMS-g-PEO Tg in the networks is a first indication of a strong crosslinked structure and incomplete phase segregation. In this sense, a system containing only PUUS and PDMS-g-PEO was prepared, with respect to full networks synthesis pathway. From Figure 3c only one Tg may be observed, that of PUUS, and a significant lowering in the PDMS-g-PEO melting profile intensity (7 J·g^{-1}), this being an indication for a good mixing of the surfactant with PUUS. As in the case of PUUS/PDMS-g-PEO system, Table 2 and Figure 4b indicate a general decreasing pattern of PDMS melting profile intensity with PUUS content increase, observed for all studied networks (Figures S3 and S4).

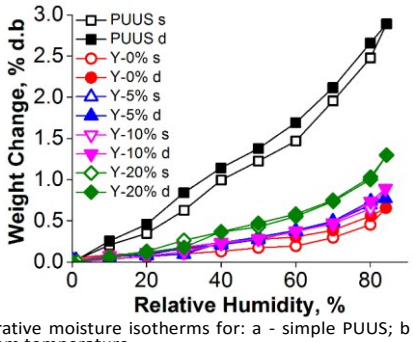

Figure 5. Illustrative moisture isotherms for: a - simple PUUS; b - Y series IPNs, recorded at room temperature.

Table 2. Thermal characteristics of studied materials extracted from DSC data.

Sample	Tg I [°C]	Tg II [°C]	Melting peak [°C]	ΔH, [J·g^{-1}]	λ_{PDMS} [%]	$\lambda_{PDMS/PUUS}$ [%]
PUUS	–65	–	–	–	–	–
PDMS-g-PEO	35	–	57	110.4	–	–
PUUS/ PDMS-g-PEO	–71	–	41	7.0	–	–
X–0%	–119	–	–43	24.0	38.0	–
X–5%	–121	–68	–43	19.8	–	32.3
X–10%	–121	–71	–43	14.2	–	23.2
X–20%	–119	–71	–46	3.4	–	5.5
Y–0%	–124	–	–42	22.1	36.1	–
Y–5%	–124	–68	–42	19.5	–	31.8
Y–10%	–125	–67	–42	19.3	–	31.5
Y–20%	–124	–67	–42	19.0	–	31.0
Z–0%	–122	–	–42	23.4	38.2	–
Z–5%	–123	–66	–42	22.8	–	37.2
Z–10%	–122	–68	–42	20.1	–	32.8
Z–20%	–124	–69	–42	19.8	–	32.3

This aspect is reflected by a decrease in PDMS crystallinity index in the networks. For this purpose, crystallinity indexes of PDMS, λ_{PDMS}, and of PDMS phase in the networks, $\lambda_{PDMS/PUUS}$, were calculated with equations 1 and 2[29] and given in Table 2:

$$\lambda_{PDMS} = (\Delta H_{PDMS}/\Delta H^{o}_{PDMS}) \cdot 100 \quad (1)$$

$$\lambda_{PDMS/PUUS} = (\Delta H_{network}/\Delta H^{o}_{PDMS}) \cdot 100 \quad (2)$$

Where ΔH^{o}_{PDMS} is the theoretical heat fusion value of PDMS (61.3 J·g^{-1} according to literature [30,31]). ΔH_{PDMS} and $\Delta H_{network}$ are the experimental heat fusion values for the pure PDMSs underlying the three networks series, $\Delta H_{X-0\%}$ = 24 J·g^{-1}, $\Delta H_{Y-0\%}$ = 22.1 J·g^{-1} and $\Delta H_{Z-0\%}$ = 23.4 J·g^{-1} (Table 2) and those corresponding to melting per gram PDMS within the IPNs, respectively. One may clearly observe from Table 2 a decrease in PDMS crystallinity in the networks as the PUUS concentration increases. A more severe reduction in the $\lambda_{PDMS/PUUS}$ ratio is recorded for the X series (Mn=70000 g·mol^{-1}) as compared to Y (Mn=230000 g·mol^{-1}) and Z (Mn=370000 g·mol^{-1}). Since crosslinking occurs at chain ends, the higher Mn values of the PDMS used in the latter two IPN series result in a lower crosslinking degree, reflected in a general decrease in Tg value corresponding to PDMS component (Tg I ranges between -119 °C and -125 °C) (Table 2). The consequences reside in increasing amorphous regions and thus reducing crystallite thickening, hence the decrease in the ΔH values within each series (Table 2).[32] Based on all observations from DSC data, one may conclude that the obtained networks exhibit a partial phase separation process.

Moisture behaviour

For proper functioning of the materials in certain applications it is necessary to ensure consistency of their characteristics of interest in different environmental conditions (i.e., temperature and humidity). In this case, as stated in the beginning, they are mainly mechanical and dielectric characteristics. While DSC analysis did not reveal significant transitions in the temperature range of -50-150 °C, which could affect the mechanical properties, it is of interest to determine the effect of moisture, which may mainly impair the dielectric properties. In order to verify this, the water vapours sorption - desorption isotherms were recorded for one of the sample series within 0-80 wt% relative humidity range, at room temperature (Figure 5). As expected, the water vapour sorption ability gradually increases as the sample is rich in polar components, from 0.65 wt% in the reference sample without PUUS (Y-0 %) to 1.29 wt% for the sample containing 20 % PUUS (Y-20 %), the sorption of pure PUUS being 2.88 wt% (Table 1S). However, sorption value for prepared IPNs remains low, which constitutes a guarantee for the properties stability. It is assumed that moisture sorption mainly is limited by the presence of siloxane on the surface of the sample which is known to have a tendency to migrate to the air interface.[33] In addition, the hysteresis is very small in all cases and the desorption runs without loss or gain of weight, the sample returning exactly to the original mass.

Mechanical testing

Besides IPNs stability and morphological aspects, the obtained films are of interest in terms of electromechanical characteristics. With respect to this, several tests were performed in order to highlight the effectiveness of achieved IPN membranes. Firstly, samples were tested by mechanical tensile and the stress-strain curves revealed, that with the increasing amount of polyurethane, the films become stiffer (see Figure 6). Thus, as is presented in Table 3, the elastic modulus increases in all cases by adding the polyurethane. The largest increase occurred in the case of PDMS with lowest molecular weight, starting from 0.2 MPa for reference sample to 1.6 MPa for sample containing 20 wt% polyurethane. This increase is assigned to the polyurethane rigidity, this having Young modulus Y=2.5 MPa, about 10 times higher than reference sample X-0%, and about 20 times higher than reference samples Y-0% and Z-0%. Furthermore, Y and Z series (Mn(Y)= 230 kg·mol^{-1} and Mn(Z)= 370 kg·mol^{-1}) have the highest strain values, the breaking occurring in the range of 600 % – 1000 % elongation. By contrast, the X series (Mn=70 kg·mol^{-1}) shows the lowest strain at break, around 100 % (Figure 6). Young modulus decreases in the three series in the order X>Y>Z as the molecular mass of the PDMS increases.

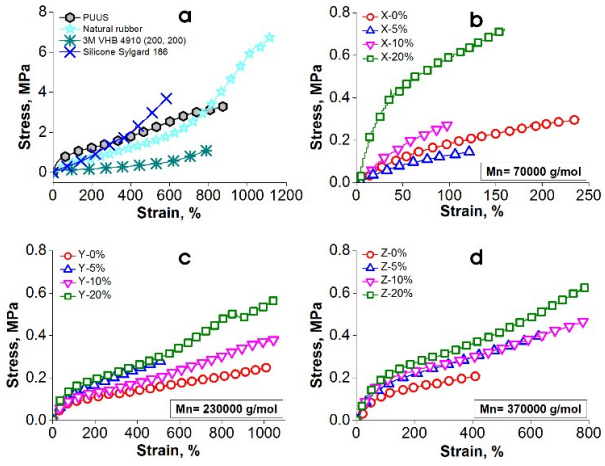

Figure 6. Stress-strain curves for: a - simple PUUS, natural rubber, VHB 4910 (200 % equibiaxially prestrained) and Sylgard 186; b, c, d – the three derived IPN series.

Table 3. The main mechanical and dielectric parameters and electromechanical actuation performance.

Sample	Young modulus[b] [MPa]	Weight [% d.b.]	Mechanical loss (100% strain)[c], [KJ·m^{-3}]	ε' at 10^0 Hz	ε' at 10^4 Hz	tan δ at 10^0 Hz	tan δ at 10^4 Hz	s_x,[d] at 5 V·µm^{-1} [%]	s_x, at 10 V·µm^{-1} [%]	s_x, at 20 V·µm^{-1} [%]	Ebd,[e] [V·µm^{-1}]
PUUS	2.5	2.9	124	12	5.9	16.40	0.030	0	0.3	1.7	44
Natural rubber	0.7	-	2	2.4	2.3	0.01	0.001	0	0.1	0.6	67
3M VHB 4910[a]	0.8	-	1	5.0	4.4	0.02	0.030	0.3	1.4	5.5	76
Sylgard 186	0.7	-	1	2.8	2.8	0.03	0.003	0.1	0.2	1.8	98
X-0%	0.2	-	2	2.9	2.9	0.13	0.010	0.1	0.2	1	124
X-5%	0.2	-	6	4.7	2.5	0.12	0.020	0.2	0.3	1.1	37
X-10%	0.6	-	6	4.7	2.4	0.26	0.010	0.1	0.4	1.5	26
X-20%	0.6	-	10	10.6	2.9	15.80	0.060	0	0.3	-	11
Y-0%	0.1	0.6	3	3.1	2.9	0.03	0.005	0.2	0.9	2.3	92
Y-5%	0.1	0.8	12	4.0	3.2	0.04	0.009	0.3	1	5.7	63
Y-10%	0.2	0.9	13	4.5	3	0.08	0.010	0.4	1.3	7.1	44
Y-20%	0.4	1.3	17	5.2	2.8	0.16	0.010	0	0.2	0.6	37
Z-0%	0.1	-	4	3.2	3.2	0.20	0.005	0.1	0.4	3.1	60
Z-5%	0.1	-	6	4.0	2.9	0.08	0.030	0.1	0.4	3.8	53
Z-10%	0.1	-	14	4.1	2.7	0.11	0.010	0.2	1.2	6.1	41
Z-20%	0.2	-	18	5.2	2.7	0.21	0.010	0	0.1	0.3	29

[a]200 % equibiaxially prestrain; [b]Young modulus at 10 % strain; [c]determined graphically by integrating the area between first stress-strain loading and unloading curve; [d]lateral actuation strain; [e]electric breakdown field.

Within each series, the modulus increases as PUUS content in the sample is greater. All these are expected results. A PDMS of high molecular weight involves a low crosslinking degree resulting in a softer material, while a high PUUS content facilitates occurrence of physical crosslinks by hydrogen bonding. In addition, stress-strain cycles were performed in order to evaluate the viscoelastic losses of materials. As Figure S6 suggests, the polyurethane film had the highest plastic deformation compared to the IPN materials. The plastic deformation of the prepared materials increases as was expected, with increasing amount of polyurethane and also with the PDMS molecular weight. Moreover, from stress-strain curves, the amounts of elastic energy dissipated during the second cycle were calculated and the obtained values reveal that, the energy loss also increases as the polyurethane quantity increases and ranges from about 3 KJ·m^{-3} for PDMS reference samples (X-0%, Y-0% and Z-0%) to 18 KJ·m^{-3} for sample Z-20% (see Table 3).

However, the three commercial dielectric elastomers investigated show lower loss values as compared with our samples. Elastic energy losses can be determined graphically by integrating the area between the loading and unloading curves as a function of time. The quicker the specimen is unloaded, the more energy is dissipated. Taking into account all this aspects, Y and Z batches showed the best mechanical behaviour regarding to use these materials as dielectric materials in actuation devices.

Dielectric measurements

The presence of urethane groups along the backbone and carboxyl groups as substituent to the carbon atom from the main chain confer polarity to the PUUS, that results in a high dielectric permittivity of this as the results from Table 3 show (ε'=12 at 1 Hz and 5.9 at 10^4 Hz). Therefore, through interpenetration of the PUUS with PDMS network it is expected to result materials with increased dielectric permittivity as compared with base PDMS (Figure 7). While the influence the PUUS content on the dielectric permittivity is clear, this increases with increasing the amount of PUUS added, it is difficult to establish a correlation between molecular weight of PDMS's used and dielectric permittivity. In general, although unnatural, it might appreciate a slightly increase of this parameter with increasing molecular weight in the case of pure crosslinked PDMS (2.9, 3.1 and 3.2 for X-0%, Y-0% and Z-0%, respectively). However, when compare PUUS-PDMS samples, those based on the lower molecular mass PDMS showed the highest dielectric permittivity values, the ranking by this criterion is X>Y>Z. In the same series, the permittivity value increases with the addition of PUUS, as otherwise it makes sense, pure PUUS having the highest value of the dielectric permittivity.

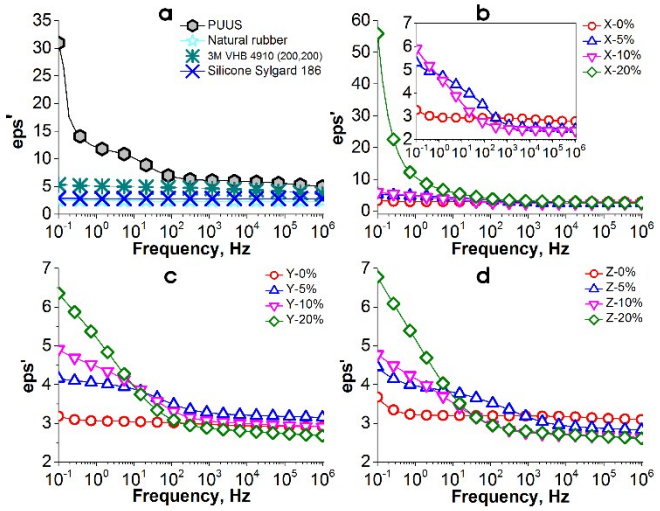

Figure 7. Dielectric spectra for: a – PUUS, natural rubber, VHB 4910 (200 % equibiaxially prestrained) and Sylgard 186; b, c, d - the samples from the three series, X, Y, and Z, respectively.

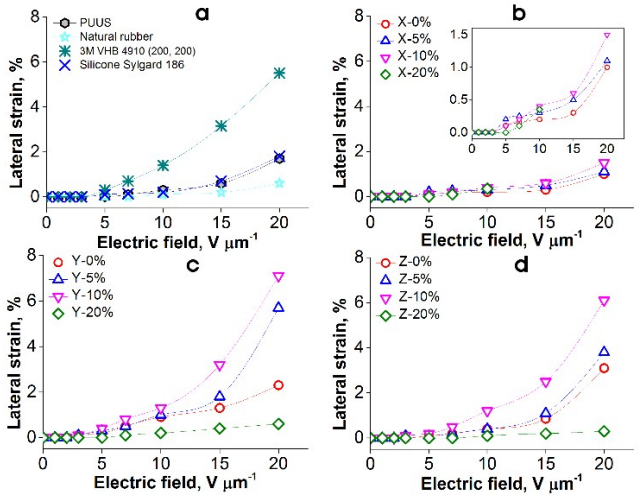

Figure 9. Lateral strain in dependence on applied electric field for: a- pure PUUS film, natural rubber, VHB 4910 (200% equibiaxially prestrained) and Sylgard 186; b, c, d-PDMS-PUUS IPN films.

On the dielectric permittivity – frequency dependence, a relaxation pick could be observed around 10^1-10^2 Hz, more pronounced as the molecular mass of PDMS increases and at an addition of 5 and 10 wt% PUUS. At low frequency, PUUS has the highest dielectric loss values, even reaching 2000 at < 0.1 Hz. The IPNs with highest PUUS content (20 wt%) also show high value, in special in the case of series X (Figure S8). However, as the frequency increases over 10 Hz, the dielectric loss stabilizes at minimum values, generally sub-unitary. A behaviour apart from other series can be noticed in the case of series Y samples in terms of dielectric loss and loss tangent (Figure S8 and S9). They show a relaxation pick little moving from 10^2 Hz at the addition of 5 % PUUS, toward less frequency as PUUS content increases (10 Hz to 20 % PUUS). The relaxation peaks are better emphasized on the tan δ –frequency curves (Figure S9). This behaviour is less visible in the other two series.

As expected, the breakdown values fall's both with increasing molecular weight of PDMS and the content of PUUS. PUUS has the lowest value for electrical breakdown field, Ebd (44 V·μm^{-1}), both compared to the other dielectric elastomers taken for comparison, and compared to the three PDMSs used as partners in building IPNs. Although the pure PDMSs showed higher Ebd, a strange behaviour has evidenced in the cases of the resulted IPNs when, by adding increasing amounts of PUUS, the resulted IPNs have sometimes values lower than its.

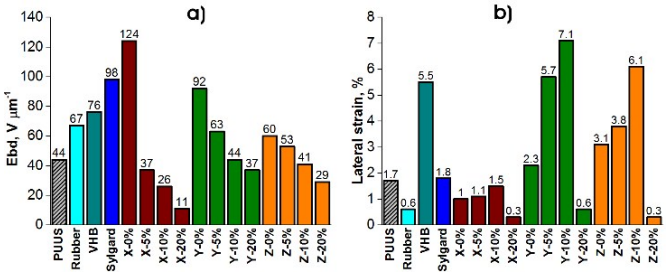

Figure 8. Graphical representation of comparative: a- Ebd and b – lateral strain values for each prepared IPN series as compared with values for pure PUUS and several commercial materials currently used as dielectric elastomers (natural rubber, acrylic VHB and siliconic Sylgard).

This trend is more pronounced in the case of X series within which, while pure PDMS has the highest value of breakdown (124 V·μm^{-1}), by the addition of PUUS, all resulting materials have values below the corresponding pure PDSM (Figure 8a). This anomaly can be attributed to surface porosity of the film which, as SEM images revealed (Figure S2), is greater as the molecular weight of the polymer is lower, like X. In this case, the higher crosslinking density makes as the solvent and condensation by-products to evaporate more slowly leaving voids mainly on the surface.

Actuation measurements

Based on mechanical and dielectric characteristics outlined above, it is expected that materials obtained present a good electromechanical response due to the combination between the mechanical chains segment motion with that related to the polarization. In general, the activation energies for different types of motion can be different, resulting in different relaxation times in the dielectric, the elastic compliance, and the electrostrictive data.[34] The electromechanical actuation was measured according to rules recently recommended by the EuroEAP society.[35] The lateral strain values, read as applied electric field increased, are showed in graphics from Figure 9 for reference samples and the three series prepared by us. The actuation values at 5, 10 and 20 V·μm^{-1} are centralized in Table 3, the hierarchy of values maintaining the same at the three voltages applied. It can be seen that this parameter increases from the series X to series Z due to increasing siloxane chain length between the crosslinking nodes and, within any given series, it increases up to an addition of 10 % PUUS; the highest values naturally are obtained at higher applied voltages. This actuation shift in the three series seems to be mainly determined by the elastic modulus whose values follow a similar model but the trend reversed (decreasing both in three sets separated by molecular weight of PDMS, as well as within each series once PUUS content increases) (Figure 8b). The samples containing 20 wt% PUUS show poor actuation although possess the highest dielectric permittivity.

Table 4. Experimental and theoretical calculated values of the electrically induced strain illustrative showed for IPNs containing 10% PUUS as compared with several commercially available dielectric elastomers.

Sample	Evaluation procedure	S_x at an applied electric field of: 5 V·µm^{-1} [%]	10 V·µm^{-1} [%]	20 V·µm^{-1} [%]
PUUS	experimental	0	0.3	1.7
	theoretical	0.1	0.6	2.3
Natural rubber	experimental	0	0.1	0.6
	theoretical	0	0.2	0.6
3M VHB 4910 (200, 200)	experimental	0.3	1.4	5.5
	theoretical	0.1	0.3	1.2
Silicone Sylgard 186	experimental	0.1	0.2	1.8
	theoretical	0.1	0.2	0.7
X-10%	experimental	0.1	0.4	1.5
	theoretical	0.1	0.4	1.8
Y-10%	experimental	0.4	1.3	7.1
	theoretical	0.4	1.5	6.4
Z-10%	experimental	0.2	1.2	6.1
	theoretical	0.4	1.6	6.7

The fact that they have higher modulus values but also poor compliance electrode, due to the surface porosity (Figure S2) of the dielectric, could explain these poor results. In general, the actuation values for samples prepared are higher than those obtained for three commercially available dielectric elastomers, among them 3M VHB seems to be the best. In actuation mode, when an electric field is applied on dielectric, the Maxwell pressure generated between the two electrodes is given by:

$$p=\varepsilon\varepsilon_0 E^2 \quad (3)$$

Where p is the electrostatic pressure across the electrodes, ε is the relative permittivity, ε_0 is the permittivity of the free space and E^2 represents the electric fields applied on electrodes.[36]
Using the linear-elasticity and boundary approximations, valid for small strains (<10%), the actuation strain in z direction (thickness) is given by:

$$s_z = -\frac{p}{Y} \quad (4)$$

where Y represents the Young modulus.[37]
Considering that the elastomer is incompressible, $Az=ct$, where A represents the aria of the electrodes, z is the thickness of the dielectric film placed between electrodes [36], thereby it can be determined the actuated thickness of the elastomer z_1:

$$z_1 = z_0 - (s_z \times z_0) \quad (5)$$

where z_0 is the elastomer thickness.
The actuated diameter of the electrodes will be:

$$d_1 = \sqrt{\frac{d_0^2 z_0}{z_1}} \quad (6)$$

where d_1 and d_0 are the initial and the final diameter of the circular electrode.
The theoretical in plane actuation (lateral actuation) s_x was calculated with the formulae:

$$s_x = \frac{d_1 - d_0}{d_0} 100 \quad (7)$$

In our calculation it was taken into account the elastic modulus for 10 % strain and the dielectric permittivity at 0.1 Hz (Table 4).

Conclusions

Original polyurethane containing tetramethyldisiloxane moiety but also pendent carboxyl groups in structure has been prepared and used in different percentages as partner with PDMS to generate hybrid siloxane-organic IPNs. A small amount of PDMS-g-PEO was added in small percentage that, besides the tetramethyldisiloxane moieties from PUUS backbone, to assure compatibilization between the two IPN incompatible partners. Although phase separation was not completely prevented, it is not a major one, especially in moderate percentages of polar components. The presence of two Tg domains suggests phase separation phenomenon occurrence but these being extremely weak is an indication of an incomplete phase segregation. As expected, by rising the content of PUUS in IPNs induces increasing moisture sorption values although these remain at low values, from 0.65 wt% in the reference sample without PUUS (Y - 0 %) to 1.29 wt% for the sample containing 20 % PUUS (Y - 20 %). The tensile test results revealed that, in all cases, with the increasing amount of polyurethane, the films become stiffer, the elastic modulus increasing. The largest increase occurred in the case of PDMS with lowest molecular weight, starting from 0.2 MPa for reference sample to 1.6 MPa for sample containing 20 wt% polyurethane. The plastic deformation also increases with increasing amount of polyurethane (which itself has the highest plastic deformation) and also with the PDMS molecular weight, as cyclic stress-strain tests showed. As expected, through interpenetration of the PUUS with PDMS networks, due to the polarity of the urethane groups and pendant carboxyl groups of the former, results in increased dielectric permittivity of the resulted materials as compared with base PDMS but decreasing in dielectric strength. However, higher dielectric permittivity value besides moderate increasing in Young modulus reflect in increasing of electrically induced actuation up to 7.1 % at 20 V·µm^{-1} in the case of the PDMS with Mn=230000 g·mol^{-1} interpenetrated with 10 wt% PUUS. At 20 wt% PUUS, all samples failed in actuation due to their accentuated surface porosity. Our samples better actuate as compared with selected commercial dielectric elastomers measured in the same conditions. The experimental values fit quite well with those theoretical calculated according to well-known relationships.

Acknowledgements

The work presented in this paper is developed in the context of the project PolyWEC (www.polywec.org, prj. ref. 309139), a FET-Energy project that is partially funded by the 7th Framework Programme of European Community and co-financed by Romanian National Authority for Scientific Research, CNCS-UEFISCDI (Contract 205EU).

Notes and references

1 R. E. Pelrine, R. D. Kornbluh, J. P. Joseph, *Sensors and Actuators A* 1998, **64**, 77-85.
2 Siegfried Bauer, in Encyclopedia of Polymeric Nanomaterials,(Eds: S. Kobayashi, K. Müllen) Springer Berlin Heidelberg, Berlin 2015, Ch. Dielectric Elastomers, 1-9.
3 R. Vertechy, G. P. P. Rosati, M. Fontana, *Journal of Vibration and Acoustics* 2014, **137**(1), 011004.
4 S. Chiba, M. Waki, K. Masuda, T. Ikoma, H. Osawa, Y. Suwa, in Design for Innovative Value Towards a Sustainable Society, (Eds: M. Matsumoto, Y. Umeda, K. Masui, S. Fukushige), Springer Netherlands 2012, Ch. Innovative Power Generation System for Harvesting Wave Energy, 1002-1007.
5 R. D. Kornbluh, J. Eckerle, B. McCoy, *SPIE Newsroom* 2011, 1-3.
6 G. Schwartz, B. C.-K. Tee, J. Mei, A. L. Appleton, D. H. Kim, H. W. & Z. Bao, *Nature Communications* 2013, **4**, 1859.
7 H. Stoyanov, M. Kollosche, S. Risse, R. Waché, G. Kofod, *Adv. Mater.* 2012, **25**, 4, 578-583.
8 S. J. Dünki, Y. S. Ko, F. A. Nüesch, D. M. Opris, *Adv. Funct. Mater.* 2015, **25**, 16, 2467-2475.
9 F. Carpi, G. Gallone, F. Galantini, D. De Rossi, *Adv. Funct. Mater.* 2008, **18**, 2, 234-241.
10 C. Tugui, M. Cazacu, L.Sacarescu, A. Bele, G. Stiubianu, C. Ursu, C. Racles, *Polymer* 2015, **77**, 312-322.
11 G. Gallone, F. Galantini, F. Carpi, *Polymer International* 2010, **59**, 3, 403-406.
12 R. D. Kornbluh, R. Pelrine, Q. Pei, S. Oh, J. Joseph, *Proc. SPIE* **3987**, *Smart Structures and Materials*, 2000 51.
13 F. B. Madsen, A. E. Daugaard, S. Hvilsted, A. L. Skov, *Macromol. Rapid Commun.* 2016 **37**, 378-413.
14 P. Brochu, Q. Pei, in Electroactivity in Polymeric Materials, (Eds: L. Rasmussen), Springer Science+Business Media, New York, 2012 Ch. 1, Dielectric Elastomers for Actuators and Artificial Muscles, 1-56.
15 S. M. Ha, W. Yuan, Q. Pei, R. Pelrine, S. Stanford, *Adv. Mater.* 2006 **18**, 7, 887-891.
16 J. Biggs, K. Danielmeier, J. Hitzbleck, J. Krause, T. Kridl, S. Nowak, E. Orselli, X. Quan, D. Schapeler, W. Sutherland, J. Wagner, *Angew. Chem. Int. Ed.* 2013 **52**, 9409-9421.
17 D. Tang, J. Zhang, D. Zhou, L. Zhao, *Journal of Materials Science*, 2005 **40**(13), 3339-3345.
18 R. Pelrine, R. Kornbluh, J. Joseph, R. Heydt, Q. Pei, S. Chiba, *Materials Science and Engineering C*, 2000 **11**, 89-100.
19 C. Tugui, G. Stiubianu, M. Iacob, C. Ursu, A. Bele, S. Vlad, M. Cazacu, *J. Mater. Chem. C*, 2015 **3**, 8963-8969.
20 J. Qingming, Z. Maosheng, S. Renjie, C. Hongxiang, *Chinese Science Bulletin*, 2006 **51**, 3.
21 H. Xiao, Z. H. Ping, J. W. Xie, T. Y. Yu, *Journal of Polymer Science: Part A: Polymer Chemistry*, 1990 **28**, 3, 585-594.
22 L. Pricop, V. Hamciuc, M. Marcu, A. Ioanid, S. Alazaroaie, *High Performance Polymers* 2005, **17**, 2, 303-312.
23 M. Cazacu, M. Marcu, *Journal of Macromolecular Science, Part A: Pure and Applied Chemistry* 1995, **32**, 7, 1019-1029.
24 C.A. Schneider, W.S. Rasband, K.W. Eliceiri, *Nature Methods* 2012, **9**, 671-675.
25 S. Zhang, Z. Ren, S. He, Y. Zhu, C. Zhu, *Spectrochimica Acta Part A Molecular and Biomolecular Spectroscopy* 2007 **66**, 1, 188-193.
26 F. Rafiemanzelat, A. Z. Fathollahi, G. Emtiazi, *Amino Acids* 2013 **42**, 2, 449-459.
27 N. Mahmood, A. U. Khan, M. S. Khan, Z. Ali, A-U. Haq, A. Wutzler, *Journal of Applied Polymer Science* 2011, **122**, 2, 1012-1018.
28 D. Rosu, L. Rosu, F. Mustata, C. D. Varganici, *Polymer Degradation and Stability* 2012, **97**, 8, 1261-1269.
29 Y. Li, Q. Ma, C. Huang, G. Liu, *Mater. Sci. (Medžiagotyra)* 2013, **19**(2), 147–151.
30 C. M. Roland, C. A. Aronson, *Polymer Bulletin* 2000, **45**, 439-445.
31 A. C. M. Kuo, in Polymer Data Handbook (Eds: J. E. Mark), Oxford University Press, 1999, Ch. Poly(methylphenylsiloxane).
32 T. Dollase, H. W. Spiess, M. Gottlieb, R. Yerushalmi-Rozen, *Europhys. Lett* 2002, **60**, 390-396.
33 E. Yilgör, E. Burgaz, E. Yurtsever, I. Yilgör, *Polymer* 2000, **41**, 3, 849-857.
34 Q. M. Zhang, J. Su, C. H. Kim, R. Ting, R. Capps, *J. Appl. Phys.* 1997, **81**, 6, 2770.
35 F. Carpi, I. Anderson, S. Bauer, G. Frediani, G. Gallone, M. Gei, C. Graff, C. Jean-Mistral, W. Kaal, G. Kofod, M. Kollosche, R. Korngluh, B. Lassen, M. Matysek, S. Michel, S. Nowak, B. O`Brien, Q. Pei, R. Pelrine, B. Rechenbach, S. Rosset, H. Shea, *Smart Materials and Structures* 2015, **24**, 10, 105025.
36 R. E. Pelrine, R. D. Kornbluh, J. P. Joseph, *Sensors and Actuators A: Physical* 1998, **64**, 1, 77-85.
37 P. Brochu, Q. Pei, *Macromolecular Rapid Communications* 2010, **31**, 1, 10-36.

The table of contents entry

Original interpenetrating polymer networks suitable for active dielectric elements in actuation devices were prepared by using a dual compatibilization pathway.

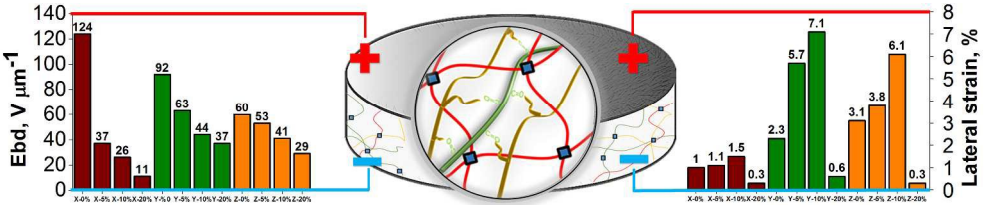

909x183mm (96 x 96 DPI)